JOURNAL OF MATERIALS SCIENCE 23 (1988) 467–474

An analysis of the creep of hot pressed silicon nitride in bending

T. FETT*, K. KELLER‡, D. MUNZ*§
*Kernforschungszentrum Karlsruhe, Institut für Material- und Festkörperforschung IV,
‡Institut für Keramik im Maschinenbau, Universität Karlsruhe, and §Universität Karlsruhe, Institut für Zuverlässigkeit und Schadenskunde im Maschinenbau, 7500 Karlsruhe, FRG

The creep behaviour of hot pressed silicon nitride is investigated in four-point-bend tests at temperatures of about 1200° C. By use of appropriate creep laws for the primary creep range as well as for the secondary range the experimental results can be well described analytically.

1. Introduction

A knowledge of the creep behaviour of ceramic materials is of importance in computing the lifetime at high temperatures. To consider failure by subcritical crack growth as well as creep crack growth one must know the time dependent stresses for all locations of the loaded structure.

To allow elementary calculations to be made a mostly pure stationary creep behaviour – expressed by a simple Norton power law – has been assumed in the literature [1–4].

For ceramics with a distinct transient creep portion a more complex procedure is necessary. This applies to hot-pressed silicon nitride (HPSN), especially MgO-doped HPSN. The creep behaviour of this ceramic will be investigated in detail.

Very often creep tests are performed as bending tests. Compared with tensile creep tests there are essential advantages in the testing procedure, but unfortunately much higher expenses in analytical evaluation. Here a general procedure to evaluate bending creep tests is presented.

2. A bending bar under creep conditions

A bending bar of thickness h and width $b = 1$ is considered. The strain rate in a fibre at the distance η from the middle axis is composed of the elastic deformation rate $\dot{\sigma}/E$ and the creep rate $\dot{\varepsilon}_c$. In agreement with Bernoulli's hypothesis the total strain rate is linearly distributed through the specimen. If $y = 2\eta/h$ is the normalized distance from the middle axis one can write

$$\dot{\varepsilon}(y) = \dot{\sigma}(y)/E + \dot{\varepsilon}_c(y) = C_1 + C_2 y \quad (1)$$

where E is the Young's modulus.

Fig. 1 shows the geometrical quantities and the strain distribution in the bending bar described by Equation 1. The first term describes a change Δl in specimen length. Only for non-symmetrical creep behaviour can $\Delta l \neq 0$ be expected. The second term causes the typical bending behaviour resulting in a pure deflection δ.

The factor C_2 is proportional to the deflection rate $\dot{\delta}$

$$C_2 \propto \dot{\delta} \quad (2)$$

C_2 can also be considered as the outer fibre bending strain $\dot{\varepsilon}^b$.

By integrating Equation 1 over the cross-section (taking into account that the integral over $\dot{\sigma}$ vanishes) one obtains

$$C_1 = \frac{1}{2}\int_{-1}^{1} \dot{\varepsilon}_c \, dy \quad (3)$$

Multiplying Equation 1 by y and repeated integration gives

$$C_2 = \frac{3}{2}\int_{-1}^{1} \dot{\varepsilon}_c y \, dy + \frac{\dot{M}}{EW} \quad (4)$$

where

$$\dot{M} = \tfrac{1}{4}h^2 \int_{-1}^{1} \dot{\sigma} y \, dy \quad (5)$$

is the rate of the bending moment, and

$$W = \tfrac{1}{6}h^2 b = \tfrac{1}{6}h^2 \quad (6)$$

is the moment of inertia.

From Equation 1 the complete stress–strain history of an arbitrarily loaded bending bar can be determined by solving the differential equation:

$$\frac{\dot{\sigma}}{E} = -\dot{\varepsilon}_c + \frac{1}{2}\int_{-1}^{1} \dot{\varepsilon}_c \, dy + \frac{3}{2} y \int_{-1}^{1} \dot{\varepsilon}_c y \, dy + \frac{6y\dot{M}}{Eh^2} \quad (7)$$

(a) For a static bending test mostly applied in lifetime measurements, it yields $\dot{M} = 0$.

(b) For cyclic bending tests one can choose $\dot{M} = \dot{M}_0 \sin(\omega t)$ with the cyclic frequency ω.

(c) A load controlled dynamic bending test is characterized by $\dot{M} =$ constant.

(d) For the deflection-rate-controlled dynamic bending test Equation 4 is simplified to read $C_2 =$ constant.

(e) Finally, for a relaxation test in Equation 4 one has to insert $C_2 = 0$.

3. Creep measurements

The result of a creep test under static load ($\dot{M} = 0$) obtained by deflection measurements is the pure bending strain rate. The outer fibre bending strain rate $\dot{\varepsilon}^b$ can be written by use of Equations 1 and 4 as

$$\dot{\varepsilon}^b = \frac{3}{2}\int_{-1}^{1} \dot{\varepsilon}_c y \, dy \quad (8)$$

0022–2461/88 $03.00 + .12

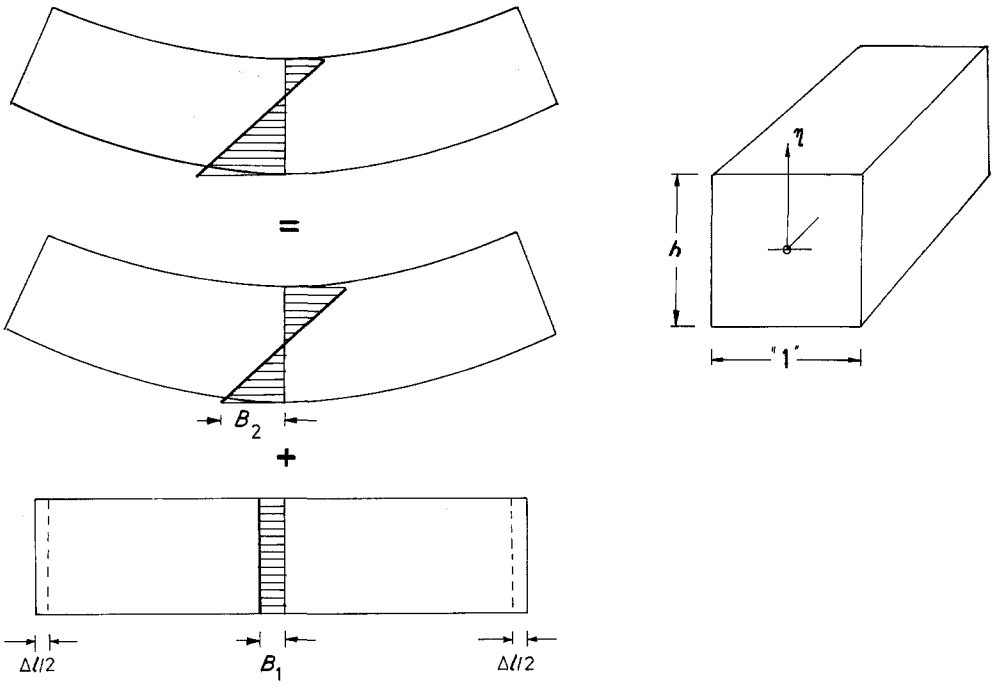

Figure 1 Creep portions and geometrical data of a bending bar.

Since this creep quantity is proportional to the deflection δ of the bending bar one can write

$$\varepsilon^b = \kappa\delta \tag{9}$$

where κ depends on the geometrical data of the testing arrangement.

If s is the distance between the inner rollers of a four-point bend test one obtains for the testing arrangement of Fig. 2

$$\kappa = \frac{4h}{s^2} \tag{10}$$

Creep measurements were performed for three different hot-pressed Si_3N_4 containing 2.5 wt % MgO, 3 wt % MgO (Ceranox NH206) and 5.5 wt % Y_2O_3 (Ceranox NH209, Annawerk, Rödenthal) at 1200 and 1400° C. Specimens (3.5 × 4.5 × 45 mm) were diamond-machined from plain parallel billets. The outer span of the four-point-bending arrangement was 40 mm, the inner span 20 mm. The deflection δ was measured directly at the specimen so that creep effects in the loading rollers and the total loading system had no influence on the measurement. As shown in Fig. 2 the displacements of the specimen were transmitted by a system of three Al_2O_3-sticks on a balance. The signal of the displacement pick up was recorded as a measure of the deflection between the inner Al_2O_3-sticks.

Fig. 3 shows some typical creep curves obtained at 1200° C. Whilst both MgO-doped materials show a nearly similar creep behaviour, for Y_2O_3-doped HPSN a significantly lower creep strain can be stated. All materials show high primary creep rates directly after loading and extended regions of stationary creep.

As an example for the effect of the bending moment Fig. 4 shows ε^b–t curves for the 3% MgO material at

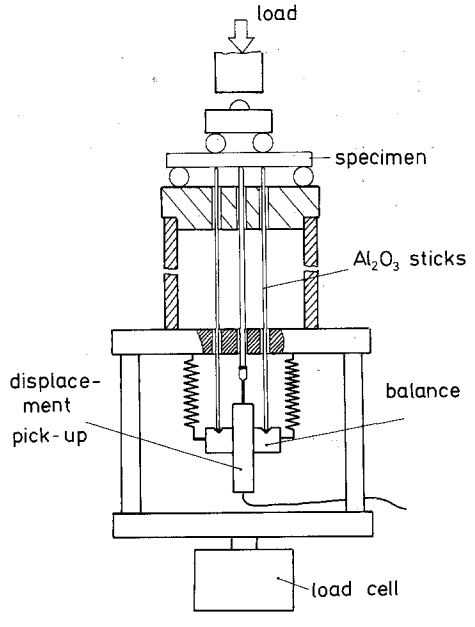

Figure 2 Direct deflection measurement for creep tests.

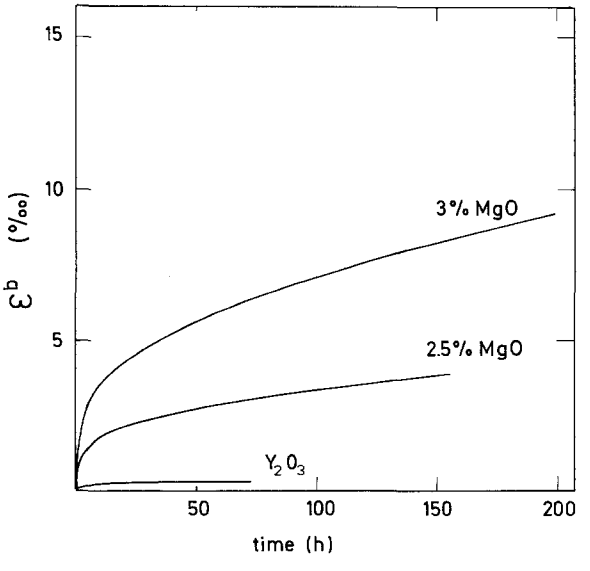

Figure 3 Typical creep curves for different HPSN, 1200° C, σ_i = M/W = 160 MPa.

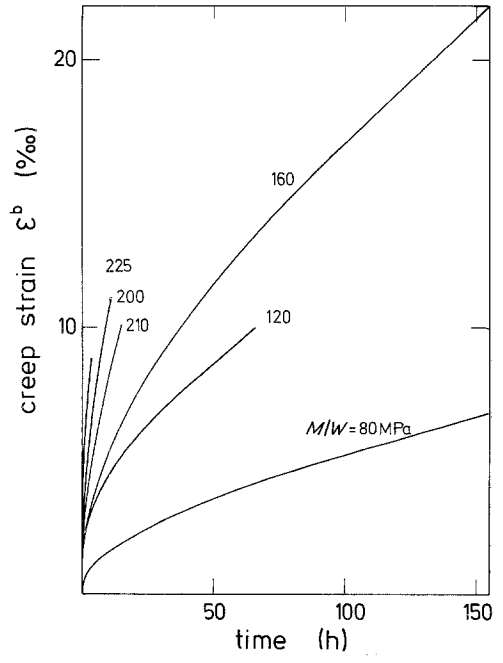

Figure 4 Creep curves obtained at 1240° C and various initial stresses for HPSN (3% MgO).

1240° C. The applied bending moment is given in terms of the elastic outer fibre stress $\sigma_i = M/W$. The creep rate $\dot{\varepsilon}^b$ decreases with increasing time and reaches a stationary value $\dot{\varepsilon}^b_s$. Similar curves have been obtained at 1200° C and for the 2.5% MgO material. Fig. 5 shows the amount of scatter for the 2.5% MgO material at 1200° C.

Up to now only the creep quantity ε^b related to pure bending has been evaluated. The second creep portion (schematically shown in Fig. 1) which is constant over the cross-section and causes a pure elongation of the specimen can be measured after the creep test.

By measuring the distance of Vickers indentations situation on the centre line on the side both before and after the creep test $\Delta l/l$ was determined taking into account the circular shape of the deformed bending bar. This creep portion is depicted in Fig. 6 as a function of the total effective creep strain ε^b.

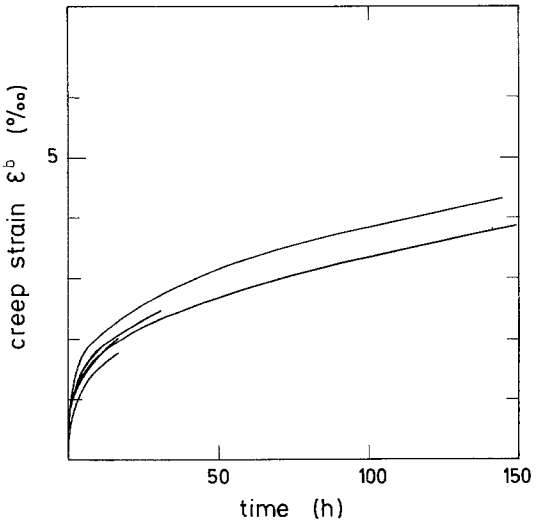

Figure 5 Creep curves for HPSN (2.5% MgO) obtained at 1200° C and identic initial stresses of 160 MPa.

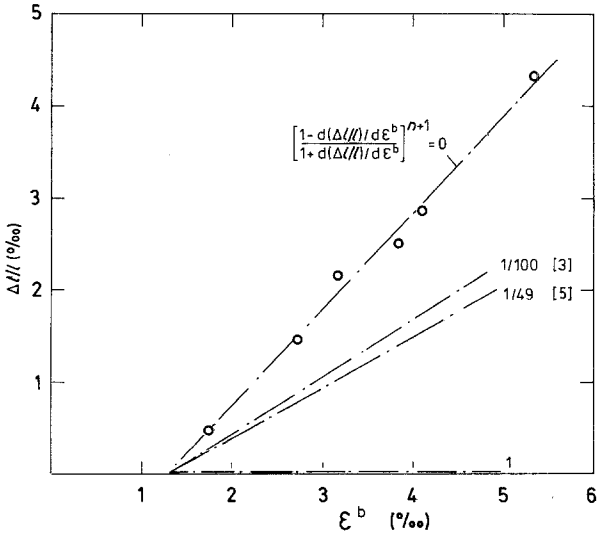

Figure 6 Elongation measurements after creep tests at 1200° C. HPSN (2.5% MgO).

4. A creep law for HPSN

Because of stress redistributions during creep tests it makes no sense to describe total creep curves by global creep equations, i.e. $\varepsilon^b \propto t^c$. The relationships become much more complicated since Equation (7) has to be solved using an appropriate local creep law.

The total creep rate $\dot{\varepsilon}_c$ is assumed to be given as the sum of the primary creep rate $\dot{\varepsilon}_p$ and the stationary part $\dot{\varepsilon}_s$

$$\dot{\varepsilon}_c = \dot{\varepsilon}_p + \dot{\varepsilon}_s \tag{11}$$

The stationary part $\dot{\varepsilon}_s$, often described by Norton's law, is modified, taking into account a non-symmetrical behaviour

$$\dot{\varepsilon}_s = D\lambda_s\sigma^n \tag{12}$$

where

$$\lambda_s = \begin{cases} 1 & \text{for } \sigma > 0 \\ \alpha_s & \text{for } \sigma < 0;\ 0 < \alpha_s < 1 \end{cases} \tag{13a}$$

takes into consideration significantly higher stationary creep rates due to tensile stresses than occurring under compressive stresses [5]. In Equation 12 the power of σ should be understood as

$$\sigma^n := |\sigma^n| \operatorname{sgn}(\sigma) \tag{13b}$$

Various relations have been proposed in the literature to describe the primary creep portion. By comparison with measured creep curves one can find the most appropriate formulation.

At first we discuss the general case that the primary creep may be governed by a non-symmetric creep law too.

Therefore, a factor of non-symmetry λ_p is assumed also for the primary creep stage

$$\lambda_p = \begin{cases} 1 & \text{for } \sigma > 0 \\ \alpha_p & \text{for } \sigma < 0;\ 0 < \alpha_p < 1 \end{cases} \tag{13c}$$

On the basis of the well-known primary creep laws proposed by Nadai [6] and McVetty [7] an appropriate combination of both laws can be found to describe primary creep of HPSN sufficiently [8]

$$\dot{\varepsilon}_p = \lambda_p B_1 \sigma^{n_1}(B_2\sigma^{n_2} - \varepsilon_p)\varepsilon_p^{-p} \tag{14}$$

In a more detailed formulation the absence of creep recovery and additional assumptions for the application of the strain-hardening rule can be taken into account by a rewritten form

$$\dot{\varepsilon}_p = \lambda_p B_1 \sigma^{n_1} F(\sigma, \varepsilon_p) \varepsilon_p^{-p} \qquad (14a)$$

where $F(\sigma, \varepsilon_p)$ equals:

$$\begin{cases} B_2\sigma^{n_2} - \varepsilon_p & \text{if } |B_2\sigma^{n_2}| > |\varepsilon_p| \text{ and } \sigma\varepsilon_p > 0 \\ 0 & \text{if } |B_2\sigma^{n_2}| < |\varepsilon_p| \text{ and } \sigma\varepsilon_p > 0 \end{cases}$$

and

$$\dot{\varepsilon}_p = 0 \qquad \text{if } \sigma\varepsilon_p < 0$$

The creep parameters in Equation 14 cannot be taken directly from bending creep curves because the stresses in the bending bar are not constant with respect to time. But they can be determined iteratively by varying their values starting with estimated values, computing the bending moment from Equations 7 and 14, and comparing the result with the measured curves.

Unfortunately, this procedure becomes extremely expensive in terms of computer time and costs. Therefore, it seems to be preferable to determine the creep parameters by approximative straightforward methods. Here the evaluation of creep parameters from asymptotic solutions of Equations 7 and 14 will be outlined in detail.

4.1. Short-time primary creep solution

For very short times the following conditions are asymptotically fulfilled:

(i) The primary creep portions, cumulated within short times, are very small compared with their maximum values and, this yields

$$\varepsilon_p \ll B_2\sigma^{n_2}$$

(ii) The stresses are equal to the initial stresses

$$\sigma = \frac{M}{W} y$$

(iii) Stationary creep portions are small compared with primary creep portions

$$\varepsilon_s \ll \varepsilon_p$$

With condition (i) Equation 14 becomes

$$\dot{\varepsilon}_p = \lambda_p B_1 B_2 \sigma^{n^*} \varepsilon_p^{-p}$$

where $n^* = n_1 + n_2$.

Inserting this into Equation 8 and integration with respect to time yields, if conditions (ii) and (iii) are taken into account,

$$\varepsilon^b \simeq \frac{3}{2} \frac{(1+p)^{(2+p)/(1+p)}}{n^* + 2(1+p)} \times (B_1B_2)^{1/(1+p)} [M/W]^{n^*/(1+p)} t^{1/(1+p)} (1 + \alpha_p) \qquad (15)$$

4.2. Long-time primary creep solution

The long-time primary creep solution is characterized by the condition $\dot{\varepsilon}_p \to 0$. With this condition the primary creep law, Equation 14a, has to be solved. For an approximative calculation an application of the simpler expression, Equation 14, is completely sufficient.

The condition of vanishing primary creep rate is equivalent to

$$\varepsilon_{p,max} = B_2\sigma^{n_2} \qquad (16)$$

The stress distribution for long times will be the stationary distribution $\sigma_\infty(y)$ given by [3, 9]

$$\sigma_\infty = \kappa H |y - y_0|^{1/n} (M/W) \qquad (17)$$

where

$$H = \frac{2n+1}{3n} \{[1 + \alpha_s^{-1/(n+1)}]/2\}^{(n+1)/n}$$

and

$$\kappa = \begin{cases} \alpha_s^{1/n} & \text{for } y_0 + y \geqslant 0 \\ -1 & \text{for } y_0 + y < 0 \end{cases}$$

$$y_0 = -[1 - \alpha_s^{1/(n+1)}]/[1 + \alpha_s^{1/(n+1)}] \qquad (18)$$

The measurable creep quantity ε^b can be obtained by inserting Equation 17 into Equation 8 and performing the integration. So it results

$$\varepsilon^b_{p,max} = \tfrac{3}{2} B_2 (M/W)^{n_2} H^{n_2} \alpha_s^m f(\alpha_s, n, n_2)$$

with

$$f(\alpha_s, n, n_2) = \frac{1}{(m+2)(m+1)} \times [(1+y_0)^{m+1}(m + 1 - y_0) + (1 - y_0)^{m+1}(m + 1 + y_0)] \qquad (19)$$

and

$$m = n_2/n$$

5. Estimation of the creep parameters

The estimation procedure for the creep parameters is schematically shown in Fig. 7. This procedure will be explained in more detail in the following sections.

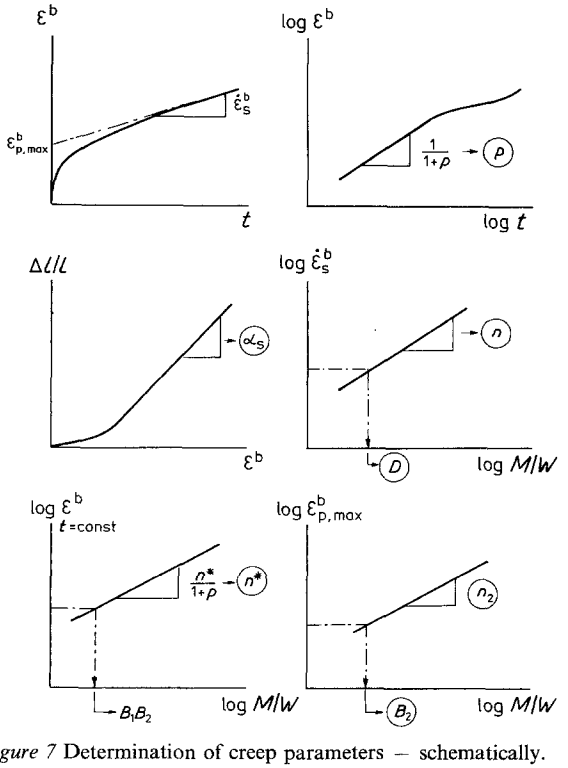

Figure 7 Determination of creep parameters – schematically.

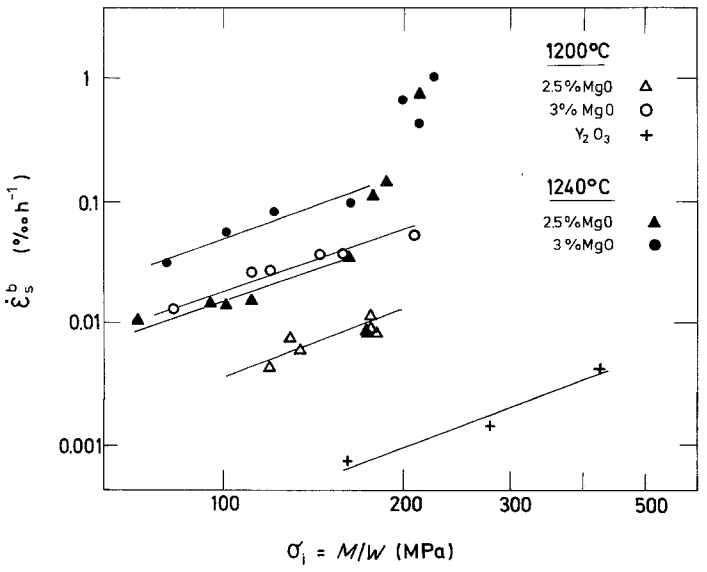

Figure 8 Minimum creep rates in dependence of the initial outer fibre stresses.

5.1. Creep parameters for stationary creep

For the stationary creep rate $\dot{\varepsilon}_s^b$ it follows by inserting Equation 12 into Equation 4 taking into account $\dot{M} = 0$

$$\dot{\varepsilon}_s^b = DH^n(M/W)^n\alpha_s \qquad (20)$$

in Fig. 8 log $\dot{\varepsilon}_s^b$ is plotted against log (M/W). For low initial outer fibre stresses $\sigma_i = M/W$ slopes of approximately $n = 2$ occur. For higher stresses an increase in the slope is found. This may not be a real effect because acceleration of creep in the tertiary creep range can occur before all stress redistributions were finished and the minimum creep rate was reached. The region near the expected point of inflection may simulate a straight line in the ε–t diagram.

To obtain the factor D from the location of the straight line in Fig. 8 α_s has to be known. To obtain α_s the elongation measurements $\Delta l/l$ have to be evaluated. Solving Equation 3 using Equation 17 gives a uniform creep quantity caused by the non-symmetry of secondary creep

$$\frac{d}{dt}(\Delta l/l)_s = -\alpha_s DH^n(M/W)^n y_0 \qquad (21)$$

Combining Equations 20 and 21 yields

$$y_0 = -\frac{d(\Delta l/l)}{d\varepsilon_s^b} \qquad (22)$$

For long times $\dot{\varepsilon}^b \to \dot{\varepsilon}_s^b$ can be used and an equation suitable to determine α_s follows

$$\alpha_s = \left(\frac{1 + y_0}{1 - y_0}\right)^{n+1} = \lim_{t\to\infty}\left[\frac{1 - d(\Delta l/l)/d\varepsilon}{1 + d(\Delta l/l)/d\varepsilon}\right]^{n+1} \qquad (23)$$

The slope in Fig. 6 leads to a neglectable creep in compression

$$\alpha_s \cong 0$$

From the literature coefficients resulting from creep rate measurements in the stationary creep range were found to be

$$\alpha_s = 1/7^n = 1/49 \qquad [5]$$

$$\alpha_s = 1/10^n = 1/100 \qquad [3]$$

Now the factor D can be obtained from Equation (20), with

$$H^n\alpha_s = \frac{2n + 1}{3n}2^{-n-1}$$

for $\alpha_s = 0$.

From the temperature dependencies in Fig. 8 activation energies of $Q = 115\,\text{kcal mol}^{-1}$ for HPSN (3% MgO) and $Q = 150\,\text{kcal mol}^{-1}$ for HPSN (2.5% MgO) can be concluded.

5.2. Creep parameters for primary creep

For short creep times the total creep strain is predominantly caused by primary creep. In this region no

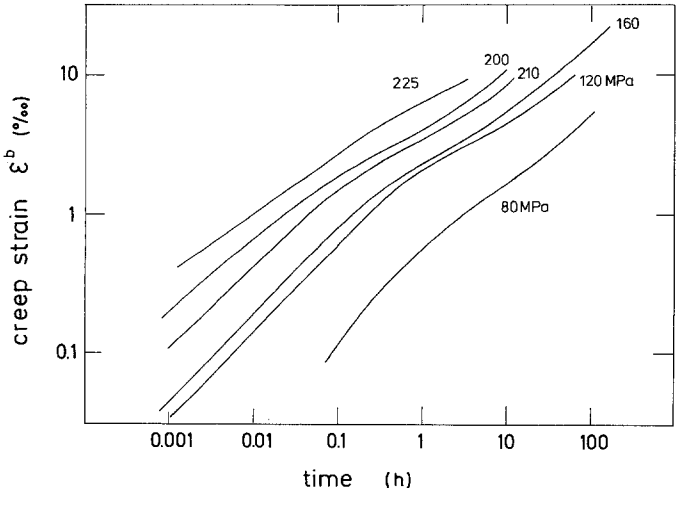

Figure 9 Log–log representation of the creep curves shown in Fig. 4.

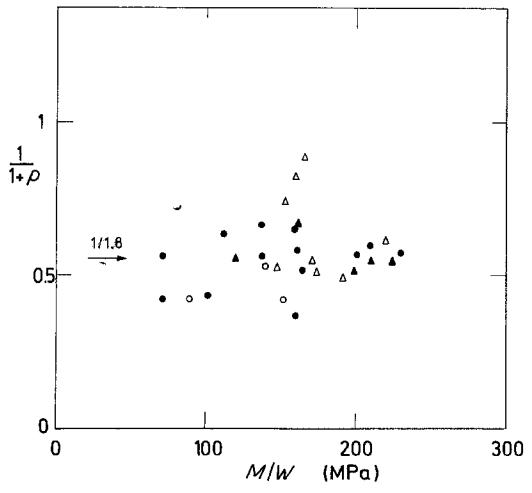

Figure 10 Slopes of the curves log ε^b against log M/W. (○) 3% MgO, 1200° C, (●) 3% MgO, 1240° C, (△) 2.5% MgO, 1200° C, (▲) 2.5%, MgO, 1240° C.

extension $\Delta l/l$ and consequently no non-symmetry are evident from Fig. 6. This gives rise to the assumption that non-symmetry will only be caused by secondary creep. Therefore $\alpha_p = 1$ was used. The small contribution of $\dot{\varepsilon}_s t$ in the primary creep range with $\alpha_s < 1$ is neglected.

By plotting log (ε_p^b) against log (t), as shown in Fig. 9 for HPSN (3% MgO), the exponent p can be determined from the slope in the linear part at low strains.

In Fig. 10 the slopes for all tests for both materials are plotted against M/W. There is a large scatter but, as expected from Equation 15, no significant effect of M/W. An average value of $p = 0.8$ is obtained from Fig. 10. From a diagram log (ε^b) against log (M/W) for a short time (Fig. 11), the exponent $n^*/(1 + p)$ can be evaluated. From all measurements a value of about 3.1 can be concluded. With a mean value of $p = 0.8$ one obtains $n^* = 5.6$ for the exponent characterizing initial primary creep.

$B_1 B_2$ can be evaluated from the intersection of the

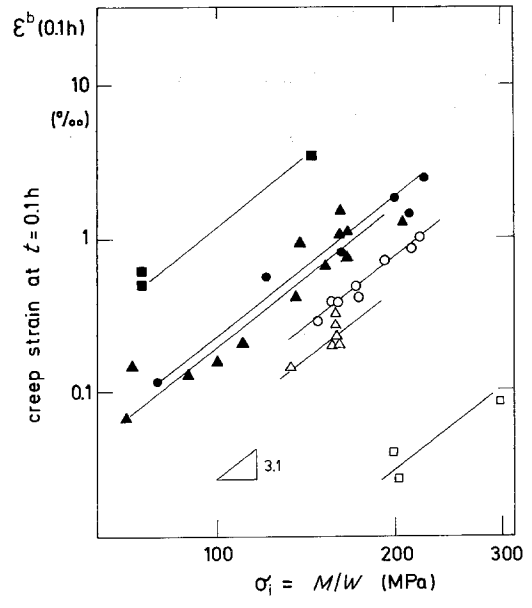

Figure 11 Creep strains at a fixed short time (0.1 h) against the initial outer fibre stress. HPSN (2.5% MgO); (□) 1100° C, (△) 1200° C, (▲) 1240° C, (■) 1300° C. HPSN (3% MgO); (○) 1200° C, (●) 1240° C.

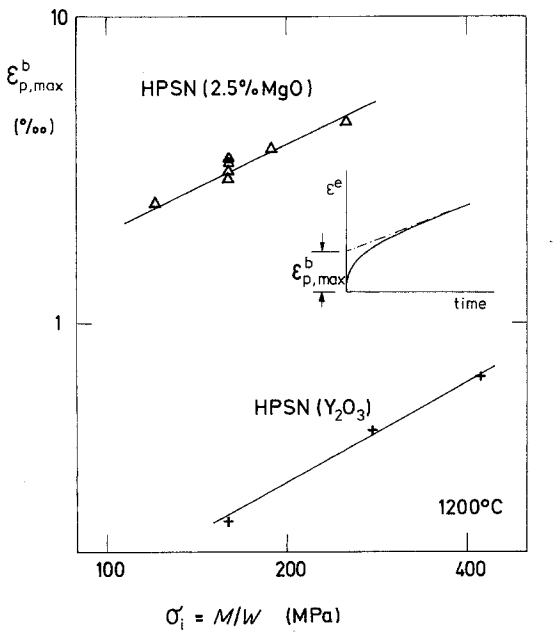

Figure 12 Total primary creep portion ε_p^b measured at 1200° C in dependence of the initial outer fibre stress.

straight lines with the ordinate in Fig. 11 if α_p is known. For the investigated materials $\alpha_p = 1$ was used.

By plotting log $(\varepsilon_p^b)_{max}$ against log (M/W) using Equation 19 from the slope of the regression line the exponent n_2 can be evaluated in principle. If α_s is known also the coefficient B_2 can be evaluated from the intersection with the ordinate.

Unfortunately, the secondary creep rate $\dot{\varepsilon}_s^b$ is not constant during the creep test because the acting stresses change from $\sigma_i = M/W$ at the beginning to $\sigma_\infty < \sigma_i$ for long times. Due to this fact, the indentification of the correct value $\varepsilon^b_{p,max}$ with the quantity coming out by an extrapolation of the final slope as shown in Fig. 12 will only be a rough estimation.

All evaluated creep parameters are given in Table I.

6. Applications

As all creep parameters are known, it is possible now

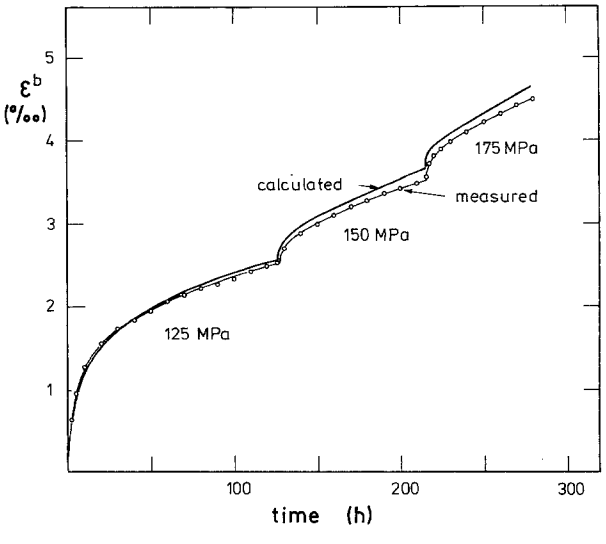

Figure 13 Calculated and measured creep strain ε_p^b for a load changing test.

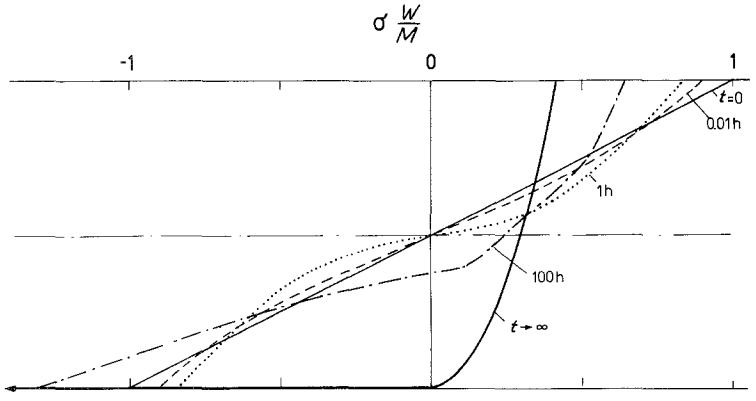

Figure 14 Time development of the stress distribution in a bending bar.

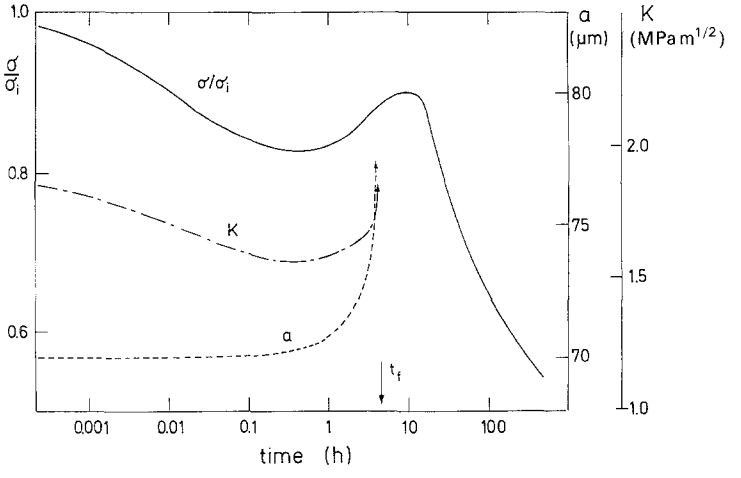

Figure 15 Time dependent outer fibre stress and development of a surface crack.

to calculate the total stress–strain behaviour of arbitrarily loaded bending bars by solving Equation 7. Two examples of application will be briefly considered here.

6.1. Example 1: Load-change experiments

In case of a static four-point bending test the load was increased stepwise. The following load history has been chosen: M/W = 125 MPa for 125 h, 150 MPa for 90 h and 175 MPa for 60 h. In a computer program Equation 3 was solved under these conditions. The data were taken from Table I for HPSN (2.5% MgO). Fig. 13 shows as the result the effective outer fibre creep strain ε_c^b against time. In addition a creep test was performed for HPSN (2.5% MgO) with the described load history. The measured data are entered as circles in Fig. 13. The agreement is satisfactory if one takes into account the usual scattering in creep tests.

6.2. Example 2: Time-dependent stress distributions

For the same material a static bending test under an initial bending stress M/W = 225 MPa was computed by solution of Equation 7, to determine the stresses at all locations of the bending beam for all times. Fig. 14 represents the time-dependent stress distributions starting with the elastic one at the moment of loading (t = 0). With increasing time the stresses become reduced at the tensile surface and the neutral axis

TABLE I

	HPSN (3% MgO)	HPSN (2.5% MgO)	HPSN (Y_2O_3)
Q (kcal mol^{-1})	115	150	–
p	0.8	0.8	–
n*	5.6	5.6	–
n_2	–	1	1
B_1(1200° C) (MPa, h)	–	1.3×10^{-13}	–
B_2(1200° C) (MPa^{-1})	–	1.4×10^{-5}	–
n	2	2	2
D(1200° C) (MPa^{-2} h^{-1})	7.1×10^{-9}	$1{\cdot}4 \times 10^{-9}$	1.06×10^{-10}
D(1240° C) (MPa^{-2} h^{-1})	1.8×10^{-8}	5.6×10^{-9}	–
B_1B_2 (MPa, h)			
1100° C	–	1.4×10^{-20}	–
1200° C	4.5×10^{-18}	1.8×10^{-18}	–
1240° C	2.7×10^{-17}	1.9×10^{-17}	–
1300° C	–	5.2×10^{-16}	–

Q denotes the activation energy for secondary creep.

shifts to the compressive surface. Here the influence of non-symmetric creep behaviour becomes evident. The stress distribution for an infinite time can be obtained from Equation 17 in a closed form.

In Fig. 15 the outer fibre stress for $y = 1$ (normalized to its initial value) is shown as a function of time after loading. The value $\sigma/\sigma_i = 1$ corresponds to the initial (elastic) stress distribution.

7. Summary

In this investigation the creep behaviour of HPSN in four-point-bend tests is analysed. The global deformation of the specimens can be well described by an appropriate creep law taking into account transient and stationary creep.

For special asymptotic cases the creep law can be integrated over the whole bending bar and relations between the local creep state and the global deformations are found. By these asymptotic solutions it is possible to determine in a straight forward manner from the experiments most parameters of the assumed creep law.

The stationary creep portion yields a Norton exponent of $n = 2$. Non-symmetric effects were examined by measuring the expansion of the specimen after the creep test. From these measurements it was concluded that stationary creep under compressive stresses must be negligible.

References

1. S. TIMOSHENKO, "Strength of Materials" Part II, "Advanced Theory and Problems (Princeton, van Nostrand, 1968).
2. F. K. G. ODQVIST and J. HULT, "Kriechfestigkeit metallischer Werkstoffe", (Springer-Verlag, Berlin/Göttingen/Heidelberg, 1962).
3. H. COHRT, G. GRATHWOHL and F. THÜMMLER, *Res. Mechanica Lett.* **1** (1981) 159.
4. T. FETT, ESA-TT-825, June 1984, European Space Agency.
5. F. F. LANGE, in "Progress in nitrogen ceramics", edited by F. L. Riley, (Martinus Nijhoff Publications, The Hague, 1983) p. 467.
6. A. NADAI, in S. Timoshenko Anniversary Volume (McMillan, New York, 1938).
7. P. G. McVETTY, *Mech. Eng.* **56** (1934) 149.
8. T. FETT, G. HIMSOLT and D. MUNZ, *Advanced Ceram. Mater.* **1** (1986) 179.
9. T. FETT, *Res. Mechanica* **18** (1986) 95.

Received 8 October 1986
and accepted 15 May 1987